

# Contextual Isotope Ranking Criteria for Peak Identification in Gamma Spectroscopy Using a Large Database

Alexis Aguilar-Arevalo, Xavier Bertou, Carles Canet, Miguel A. Cruz-Pérez, Alexander Deisting, Adriana Dias, Juan Carlos D'Olive, J. Francisco Favela-Pérez, Estela A. Garcés, Adiv González Muñoz, Jaime Octavio Guerra-Pulido, Javier Mancera-Alejandrez, Daniel José Marín-Lámbarri, Mauricio Martínez-Montero, Jocelyn Monroe, Sean Paling, Simon Peeters, Paul R. Scovell, Cenk Türkoğlu, Eric Vázquez-Jáuregui, Joseph Walding

**Abstract**—Isotope identification is a recurrent problem in  $\gamma$  spectroscopy with high purity germanium detectors. In this work, new strategies are introduced to facilitate this type of analysis. Five criteria are used to identify the parent isotopes making a query on a large database of  $\gamma$ -lines from a multitude of isotopes producing an output list whose entries are sorted so that the  $\gamma$ -lines with the highest chance of being present in a sample are placed at the top. A metric to evaluate the performance of the different criteria is introduced and used to compare them. Two of the criteria are found to be superior than the others: one based on fuzzy logic, and another that makes use of the  $\gamma$  relative emission probabilities. A program called *histoGe* implements these criteria using a SQLite database containing the  $\gamma$ -lines of isotopes which was parsed from WWW Table of Radioactive Isotopes. *histoGe* is Free Software and is provided along with the database so they can be used to analyze spectra obtained with generic  $\gamma$ -ray detectors.

**Index Terms**—Gamma-ray spectroscopy, Heuristic algorithms, Isotope identification, Ranking

## I. INTRODUCTION

This work is supported by the STFC Global Challenges Research Fund (Foundation Awards, Grant ST/R002908/1 and Translation Awards, Grant EP/T015586/1), DGAPA UNAM grants PAPIIT-IT100420 and PAPIIT-IN108020, CONACYT grants CB-240666 and A1-S-8960. M. A. Cruz-Pérez acknowledges the support of “Programa de Posgrado en Ciencias de la Tierra at Universidad Nacional Autónoma de México.”

A. Aguilar-Arevalo, J. C. D'Olive, J. F. Favela-Pérez, J. O. Guerra-Pulido, and M. Martínez Montero are with Instituto de Ciencias Nucleares, Universidad Nacional Autónoma de México, Coyoacán, CDMX, México, C.P. 04510 (e-mails: francisco.favela@correo.nucleares.unam.mx, jaime.guerra@correo.nucleares.unam.mx, mauricio.martinez@nucleares.unam.mx).

X. Bertou and J. F. Favela-Pérez are with Centro Atómico Bariloche, CNEA/CONICET/IB, Bariloche, Argentina.

A. Deisting, A. Dias, J. Monroe, and J. Walding are with Royal Holloway, University of London, Egham Hill, United Kingdom.

E. A. Garcés, A. González Muñoz, D. J. Marín-Lámbarri, and E. Vázquez-Jáuregui are with Instituto de Física, Universidad Nacional Autónoma de México, A. P. 20-364, México D. F. 01000, Mexico.

C. Canet and M. A. Cruz-Pérez are with Centro de Ciencias de la Atmósfera. Universidad Nacional Autónoma de México, Ciudad Universitaria, Coyoacán, 04510, Ciudad de México, Mexico.

J. Mancera-Alejandrez is with Facultad de Ingeniería, Universidad Nacional Autónoma de México, México.

S. Paling and P. R. Scovell are with Boulby Underground Laboratory, Boulby Mine, Saltburn-by-the-Sea, United Kingdom.

S. Peeters and C. Türkoğlu are with Department of Physics and Astronomy, University of Sussex, Brighton, United Kingdom.

C. Canet is also with Instituto de Geofísica, Universidad Nacional Autónoma de México, Ciudad Universitaria, Coyoacán 04510, Ciudad de México, México.

**G**AMMA ray spectroscopy commonly uses High Purity Germanium Detectors (HPGe) to acquire the energy spectra of samples with a varied isotopic composition. Analyzing and identifying the isotopes present in the sample is a challenging problem given the multitude of gamma lines from which to choose. Thus, computational tools are needed to analyze a spectrum and extract useful information [1], [2]. Many programs have been written to make these calculations in the past [3]–[10]. However, just a few provide the capability to identify isotopes from a given spectrum. Some previous attempts have been made to perform that identification using a relational database, for example: Hyperlab [4] has a functionality to make a “graphical iteration process” followed by a procedure to solve iteratively an “identification matrix”, however, no documentation about the method nor reports on its identification accuracy are provided for this software. GammaLab [5] uses a database called “NUCDATA” which includes information “for quick calculations for 408 radioisotopes” [11], however, it is limited in extension in comparison to other well-known databases [12]–[14] and it does not present a study about its accuracy and its real capability of identifying isotopes in a sample. ASPRO-NUC [15] has a wide set of spectral analysis tools: peak search, deconvolution, background line and simulation, spectrum smoothing, among others. It also has algorithms to identify peaks using a database of 45,000  $\gamma$ -lines corresponding to 2200 radionuclides. However, the authors recognized that identification in this way “is hardly possible” and they opted to develop an “actual isotope library”. Sandia National Laboratories provide two programs for assisting with analyzing spectral information from nuclear radiation. *InterSpec* [16] provides multipeak fitting isotope identification capabilities as well as activity calculation considering shielding from a variety of materials. The other one is called *Peak Map* [17] which is written in C#, it considers a set of parameters such as distance from the mean and half-life penalization (among others) to assign a score to the  $\gamma$ -lines and sorts with respect to that before displaying the candidate  $\gamma$ -lines.

There are many areas in which  $\gamma$ -spectroscopy is applied, e.g., high energy physics research, environmental sciences, and food contamination. An important application lies in the control of radioactive materials crossing borders around the world, where there is a need to have instruments and methods

to identify radioactive nuclei that are potentially harmful even in small amounts. While automated analysis for this problem is desirable, a study from 2007 concluded that a “secondary analysis of spectra by a trained spectroscopist is frequently necessary” to identify isotopes through their  $\gamma$ -lines [18]. Since then, new techniques have been explored to make automated isotope identification more reliable independently of the field of application, to mention a few: swarm optimization [19], Fischer linear discriminant analysis [20], Bayesian statistics approach [21], [22], neural networks (NN) [23]–[29], hybrid fuzzy-genetic algorithms [30]. Some of these methods have been used to perform automated peak identification [31]. There are also developments, using the GEANT4 toolkit, for providing training data to machine learning models [32]. Herein, new methods have been proposed, implemented, and tested using the *histoGe* code [33], a Free Software (GNU Public License [34]) with many features that are described in its User’s Manual [35].

This work deals with the  $\gamma$ -line identification problem in a manner similar to what a search engine does when presenting the results of a query. It assigns a numerical value called “rank value” (RV) to each candidate  $\gamma$ -line that may explain the presence of the peak in a spectrum.

Five criteria to identify peaks are presented, some of them are based on simple counting while others use more complex calculations, e.g., Mamdani’s fuzzy inference system (FIS). Known  $\gamma$  spectra were identified using the proposed criteria and their performance was evaluated using an *ad hoc* metric.

This work has been developed as an effort to support the research and educational activities that will be carried out at the Laboratorio Subterráneo de Mineral del Chico (LABChico), which will be located inside a decommissioned silver mine at the Comarca Minera, Hidalgo, México, inside the UNESCO Global Geopark [36]. LABChico will host HPGe to conduct studies of low radioactivity in water, soils, and products intended for human consumption, aiming to develop techniques to signal the presence of lead in drinking water. At the same time, it will serve as a training hub for students and researchers interested in radiation detectors, techniques for particle and astroparticle physics experiments, geology and mine engineering, among other areas. The *histoGe* computational software was developed as an effort to facilitate  $\gamma$ -ray spectroscopy and to identify isotopes from recorded spectra inside the laboratory. Technical details about its implementation and capabilities, how to use it, and its database of *histoGe* are described in the user’s manual [35].

This paper is organized as follows: in section II, the methodology used to identify isotopes and a brief explanation of the operation of the program and some key concepts are presented; in section III, five criteria to find the most suitable  $\gamma$ -lines that can be responsible for the peaks observed in the spectra are described; in section IV, the experimental setup is described; in section V four cases are studied: one is an example of how the general method works, the second one analyzed the spectra obtained with point-like radioactive sources through the Nuclear Sciences Institute HPGe (ICN-HPGe) detector, the third example is the analysis of spectra of some samples of rocks and water and the fourth example

presents the identification of isotopes using a spectrum taken from the literature. The last section shows the conclusions of this work.

## II. METHODOLOGICAL APPROACH

The *histoGe* software is written in Python 3 [37] and can run practically in any of the mainstream operating systems available nowadays. The basic process of line sorting used in *histoGe* is depicted in Figure 1. Energy query ranges are determined by either processing an experimental spectrum to find peaks, or by hand. *histoGe* uses a Savitzki-Golay filter [38] to smooth out spectra, detect the peaks and generate these query ranges. The width of the query ranges contains information about the resolution of the detector.

An *info* file [35] contains the energy query ranges associated with each peak. Once the file has been read, a query to the database is performed for each peak. As a result, a set of lists, one list per interval, are obtained from those queries. The lists contain information of all  $\gamma$ -lines that can be located inside the specified energy ranges. Once the RVs are calculated, each  $\gamma$ -line list is sorted and printed on the screen or stored in a text file (figure 1). The ranking operation calculates and assigns to each  $\gamma$ -line the RV used for sorting in descending order depending on the criterion (section III describes them in detail). This RV, or score, can be constructed so as to take into consideration global aspects of the spectrum, such as, for example, the possibility that a given isotope or decay chain may be responsible for several peaks, bringing context into the analysis. Once a RV has been assigned to all the  $\gamma$ -line candidates under the peaks of interest, they are sorted with respect to the other candidates within the same peak (locally), positioning the best candidates at the top of the list. Positions span from 0 to the number of the  $\gamma$ -lines found in the query minus one. A position close to 0 indicates a high preference for the  $\gamma$ -line to explain features present in the spectrum. Although all criteria need an *info* file, not all criteria require the spectrum. This general procedure is schematically represented in figure 2.

The ranking methods can be classified in three broad categories according the way the RV is calculated. Those where the RV is calculated for each  $\gamma$ -line individually without considering the other  $\gamma$ -lines of the same isotope found for the other peaks (III-A), those in which the RV is calculated for each isotope using all the  $\gamma$ -lines found in all peaks (III-B, III-C, and III-D) and those in which the RV takes into account all isotopes in the decay chains (III-E). Depending on the category to which a criterion belongs to, the RV is assigned to a  $\gamma$ -line, or to all  $\gamma$ -lines of an isotope, or to all  $\gamma$ -lines of all isotopes in a chain, correspondingly.

The whole operation is based on a local database (LDB) [39] (11 MB of disk space) that was constructed in part from the one accessible in [12]. Additional data was computed and added to have enough information to be used with the ranking criteria such as decay chains and normalized emission probabilities [35]. The total number of entries in the LDB is 92453, which is 226 times larger in comparison to [11] and more than twice the used in [15]. The database entry ( $\gamma$ -line) with the highest energy belongs to  $^{20}\text{Na}$  with 11258.9

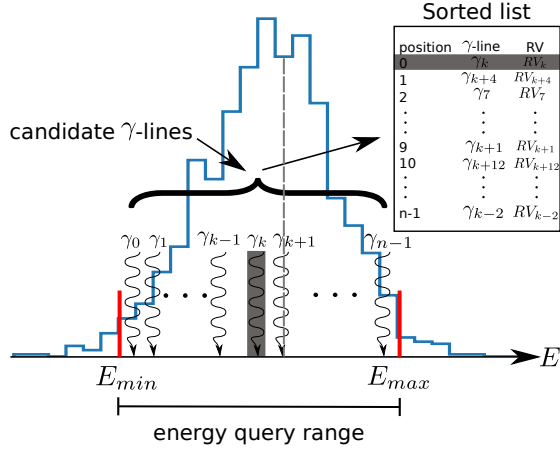


Fig. 1: Graphical description of the basic process. In general, the RV is criterion dependent which normally involves other peaks. Note that the  $\gamma$ -line closest to the peak mean is not at the top positions because sorting depends of the RV.

keV. Figure 3 shows the energy distribution of  $\gamma$ -lines in the LDB. There is an apparent under representation in the vicinity of 511 keV ( $\approx 50\%$ ). This might indicate a systematic over-subtraction of positron annihilation backgrounds in the reported measurements.

Using a large database introduces a problem to peak identification because peaks in a spectrum could be explained by many  $\gamma$ -lines, even if the peak has a narrow width. The ranking criteria presented in Section III aim to overcome this issue.

### III. RANKING CRITERIA

Ten criteria were originally designed to identify  $\gamma$ -lines from potential isotopes that could be present in a sample using the peaks found in its  $\gamma$  spectrum. They were labeled arbitrarily from A to J, however, only the most significant are reported here using their original names and codes. Information about all the methods is reported in the `histoGe's` User Manual [35]. The criteria can be applied individually or in combinations in arbitrary order.

These criteria differ from other previously reported methods in how they utilize the information such as the emission probability (EP), the relative emission probability (REP), the ratio between the number of peaks identified in the spectrum and the number of peaks found in the database for certain isotopes, among others. Each criterion has merit by itself, but they can be combined to obtain better results. Before the analysis begins, the spectra must be properly calibrated to obtain reliable results.

The criteria described in this work, their code and their ranking category are listed in table I.

When two gamma lines in the same peak get the same RV, other criteria are used as tiebreakers to decide in favor of one of them, e.g., for criterion F, criterion E is used and if the tie persists, then, criterion D is used. For criterion H,  $RMSE_{mod}$  and criterion F were used. Next, a description of each criterion is given.

TABLE I: CRITERIA NAME, CODE, RANKING CATEGORY AND THE SECTION WHERE EACH IS DESCRIBED.

Name	Code	Ranking category	Section
$\gamma$ -line coincidence probability	B	$\gamma$ -line	III-A
Improved Peak Explanation Power	E	isotope	III-B
Relative Emission Probability (REP)	F	isotope	III-C
Fuzzy logic	H	isotope	III-D
Decay chain using REP	J	chain	III-E

#### A. $\gamma$ -line coincidence probability

The distance  $d$  (in keV) from the peak mean to each of the  $\gamma$ -lines is used to calculate the probability ( $P_G$ ) that the peak can be explained by a  $\gamma$ -line. This is done using the cumulative distribution function (CDF) for the Gaussian distribution:

$$P_G(d, \mu = 0, \sigma) = 2\text{CDF}(-|d|, 0, \sigma) \quad (1)$$

where  $\mu$  is the mean of the CDF and  $\sigma$  is the peak's standard deviation obtained from a Gaussian fit. The RV is assigned directly to each  $\gamma$ -line and it is given by equation (1). The  $\gamma$ -lines are then sorted according to their RVs.

#### B. Improved Peak Explanation Power

A single parent isotope could have multiple  $\gamma$ -lines appearing as peaks in a spectrum. Every time a  $\gamma$ -line of a particular isotope is matched with a peak, the chance that the isotope is present in the sample is increased, making it more suitable to explain the spectrum as a whole. The RV is calculated as the ratio of the number of  $\gamma$ -lines from a given isotope that fall within the peaks of the spectrum, to the number of  $\gamma$ -lines from that isotope expected in the whole range of the spectrum (from the first to the last peak). The RV is in the semi-closed interval (0,1] and sorting is done in descending order.

#### C. Relative Emission Probability (REP)

The REP was calculated and included in the LDB for each  $\gamma$ -line. This had to be done since many of the entries had non-numeric or missing EP values. When not available, EP were set to the minimum EP for the isotope [35]. Using the REP allows to associate a set of  $\gamma$ -lines with their respective parent isotopes knowing that, for a given isotope, the REP of its  $\gamma$ -lines should add up to 1 [35].

The RV is calculated as the sum of the REP of those  $\gamma$ -lines found in the queries for a particular isotope. This method also gives rank values in the (0,1] and they are sorted in descending order.

#### D. Ranking With a Fuzzy Inference System

Fuzzy logic [40] was used to compose a more powerful RV from the combination of three inputs. It is a method to formalize "approximate" reasoning and it is a tool to treat uncertainty and vagueness. Unlike classical logic, where propositions can only be true or false; propositions in fuzzy

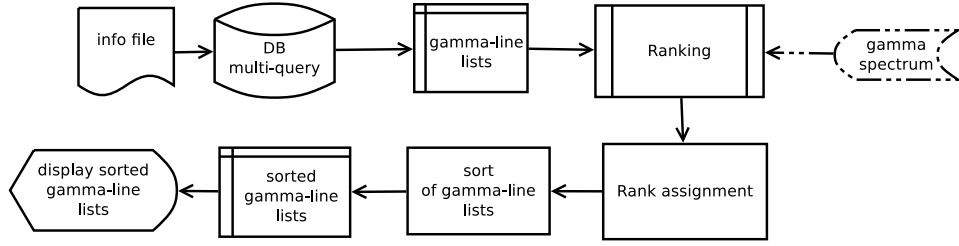


Fig. 2: Flowchart of the processing done for a given info file. Some ranking operations may need extra information not present in the `info` file such as the gamma spectrum.

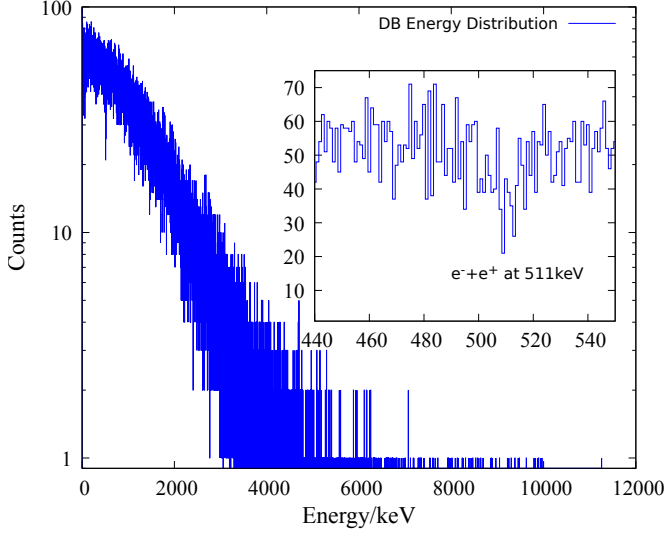


Fig. 3: Energy distribution of the entries in the LDB in 1 keV bins, note the presence of the over-depleted zone (close to 511 keV) shown more clearly at the insert.

logic can have a degree of truth between 0 and 1 [41]. A fuzzy inference system (FIS) performs a deductive inference through IF-THEN rules with fuzzy sets [42]. A well known and straight forward way to implement a FIS is through the Mamdani's inference [43]. The steps to perform this type of inference are: fuzzification of the inputs; inference, which is divided in: calculation of the antecedents, implication and aggregation of rules; and finally, defuzzification via the centroid method [41] which was used to convert a fuzzy output to a crisp number, this value is used as a RV.

Three inputs (antecedents) and one output (consequent) were used in the FIS designed to identify and rank the isotopes. The inputs of the FIS are: a "modified Root Mean Square Error" ( $RMSE_{Mod}$ ), the peak ratio defined as  $\frac{P_r}{P_T}$  where  $P_r$  is the number of peaks explained by the isotope and  $P_T$  is the total number  $\gamma$ -lines within the spectrum's range, and the REP ( $I_{gR}$ ); the output is a value between 0 and 1 and, in this context, it will be called "Affinity". It reflects the degree to which a set of  $\gamma$ -lines can be considered to belong to a particular isotope.

The  $RMSE_{Mod}$  is defined using some statistical methods to analyze  $\gamma$ -ray spectra presented by Gilmore [1] such as the net area of a peak  $A = G - B$ , where  $G$  is the peak's integral

and  $B$  is the estimated background under the peak, together with the REP. Then,  $RMSE_{Mod}$  is defined as:

$$RMSE_{Mod} = \frac{P_T}{P_r} \sqrt{\frac{1}{N} \sum_{i=1}^N \left[ \left( \frac{A_i}{A_T} \right) - \left( \frac{I_{g_i}}{I_{g_T}} \right) \right]^2}, \quad (2)$$

where  $N$  is the total number of peaks,  $A_i$  is the net area of the  $i$ -th peak,  $A_T$  is the sum of all the net areas,  $I_{g_i}$  is the REP of the  $i$ -th peak and  $I_{g_T}$  is the sum of the REP for all lines identified for the respective isotope. The factor  $\frac{P_T}{P_r}$  that modifies the  $RMSE$  in equation (2), was included to penalize those isotopes that explain fewer peaks of the spectrum in comparison to the expected number of peaks.

Each input has three fuzzy sets and the output has five fuzzy sets. Fuzzy sets were defined using the well-known sigmoid and Gaussian functions whose mathematical expressions are, respectively, given by:

$$f_s(x, k_o, x_o) = \frac{1}{1 + e^{-k_o(x-x_o)}}, \quad (3)$$

where  $k_o$  and  $x_o$  are the parameters of the sigmoid function, and

$$f_g(x, \sigma, \mu) = e^{\frac{-(x-\mu)^2}{2\sigma^2}}, \quad (4)$$

where  $\sigma$  and  $\mu$  are the parameters of the Gaussian function. Figure 4 shows the name, curve, the mathematical function of the fuzzy sets used in the FIS. The parameters of the fuzzy sets were established considering the designer's own knowledge about what the linguistic variables Very Low (VL), Low (L), Medium (M), High (H) or Very High (VH) could mean considering that the output hypersurface must be a monotonically increasing one.

The rules used for the inference are of the form:

$$\begin{aligned} \text{IF } x_1 \text{ is } RMSE_m^k \text{ and } x_2 \text{ is PeakRatio}_n^k \text{ and } x_3 \text{ is Ig}_{R_p}^k \\ \text{THEN } y^k \text{ is Affinity}_q^k, \end{aligned}$$

where  $k$  is an index that refers to  $k$ -th rule as is shown in table II and  $m, n, p$  and  $q$  are the indices of their respective fuzzy sets which can be VL, L, M, H or VH depending on whether they are input or output fuzzy sets, as shown in figure 4. The rules used for the inference process are shown in table II. Since there are three fuzzy sets for each input, there are twenty

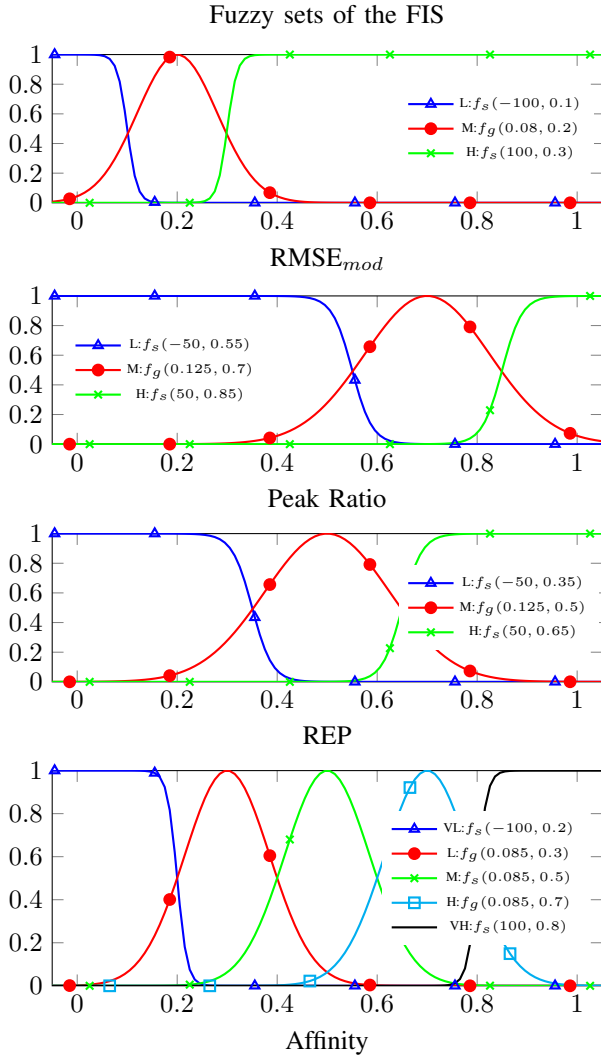


Fig. 4: Parameters of the fuzzy sets used in the FIS. Sigmoid and Gaussian functions parameters are  $f_s(x, k_o, x_o)$  and  $f_g(x, \sigma, \mu)$ , respectively. The names of the fuzzy sets are: VL is “Very Low”, L is “Low”, M is “Medium”, H is “High” and VH is “Very High”.

seven rules with their consequents chosen from five fuzzy sets. During the design of the FIS, it was decided that five output fuzzy sets were enough to categorize the combinations of the inputs.

Once the fuzzy sets are defined and the rules given, the Mamdani inference can be implemented to calculate the affinities of isotopes. All  $\gamma$ -lines that share the same parent get the same RV. They are later sorted in descending order using as a tiebreaker criterion the  $RMSE_{Mod}$ . This criterion was chosen for its simplicity and because it is already an input of the fuzzy rank method, however, other criteria such as  $Ig_R$  could be used to untie isotopes with the same RV. Efficiency corrected spectra were used, but no important improvements were observed in the results got with this method.

### E. Chain using Relative Emission Probability

In some spectra, the presence of some peaks can be due to  $\gamma$ -lines from several isotopes that are connected to each other via a decay chain. This motivates the design of a criterion that rank chains instead of isotopes alone.

For this criterion, the RV is calculated as follows: REP of the  $\gamma$ -lines found in the query ranges belonging to all the isotopes in a given chain are summed and averaged. As described in section II, the RV is assigned to all the  $\gamma$ -lines of all isotopes that belong to the chain. Sorting is done in descending order.

## IV. EXPERIMENTAL SETUP

The results in sections V-A and V-B below were obtained with spectra from a set of radioactive sealed calibration sources (Table III) and they were acquired with an EG&G-ORTEC Hyper Pure Germanium detector in the Detectors Laboratory at the Institute of Nuclear Science of the National Autonomous University of Mexico (UNAM), hereafter referred to as ICN-HPGe detector, whose characterization has been reported elsewhere [44]. The data acquisition system (DAQ) was a PX5-HPGe multi-channel analyzer (MCA) and a digital pulse processor (DPP) software analyzer provided by Amptek [45].

## V. RESULTS

### A. Example with a $^{60}\text{Co}$ sealed point-like source

As a first example, criterion F (III-C) was applied over the spectrum obtained in the ICN-UNAM from the  $^{60}\text{Co}$  point-like source reported in table III. For this test, an `info` file with two query ranges, associated with each of the two more prominent gamma lines of this isotope was used. Table IV shows the isotopes in the top 10 positions output and their corresponding gamma lines. The two energy ranges are shown in red in figure 5 as well as the 10 best candidates  $\gamma$ -lines are shown in the inserts.

Notice that, since this criterion assigns a RV per isotope,  $\gamma$ -lines from the same isotope found in the two query ranges have the same RV. For the first query range (Co60\_1: from 1160.84 keV to 1182.18 keV), the isotope  $^{60}\text{Co}$  is found at the top position by itself, but for the other one (Co60\_2: 1323.41 keV to 1340.54 keV) it is tied with  $^{53}\text{Co}$ , since all expected gamma lines are found in the query ranges for both isotopes. A tie breaking based on criterion E is effected, which places  $^{60}\text{Co}$  at the top ( $^\dagger$ ).

### B. Comparison of criteria using known $\gamma$ -sources

To compare the performance of the criteria discussed in section III, `histoGe` was employed to identify the  $\gamma$ -lines from point-like sealed sources of table III through their  $\gamma$  spectra. Table V summarizes the results, showing the positions after sorting the RV of their corresponding  $\gamma$ -lines, query ranges and  $\gamma$ -line properties. The positions given by `InterSpec` [16] are shown for comparison.

Figure 6 compares the performance of the various criteria using an *ad hoc* metric which is calculated as follows: a score (S) is assigned to each  $\gamma$ -line (table V), in the following way:

TABLE II: FIS RULES USED IN `histoGe`'S FUZZY RANK. MVL, ML, MM, MH AND MVH REFER TO THE AFFINITY OUTPUT FUZZY SETS: VERY LOW, LOW, MEDIUM, HIGH AND VERY HIGH, RESPECTIVELY.

	$RMSE_{Low}$			$RMSE_{Medium}$			$RMSE_{High}$		
	PeakRatio <sub>Low</sub>	PeakRatio <sub>Medium</sub>	PeakRatio <sub>High</sub>	PeakRatio <sub>Low</sub>	PeakRatio <sub>Medium</sub>	PeakRatio <sub>High</sub>	PeakRatio <sub>Low</sub>	PeakRatio <sub>Medium</sub>	PeakRatio <sub>High</sub>
REP <sub>Low</sub>	ML	MM	MM	MVL	ML	ML	MVL	MVL	MVL
REP <sub>Medium</sub>	MM	MH	MH	MM	MM	MH	ML	MM	MH
REP <sub>High</sub>	MVH	MVH	MVH	MH	MH	MVH	MH	MH	MH

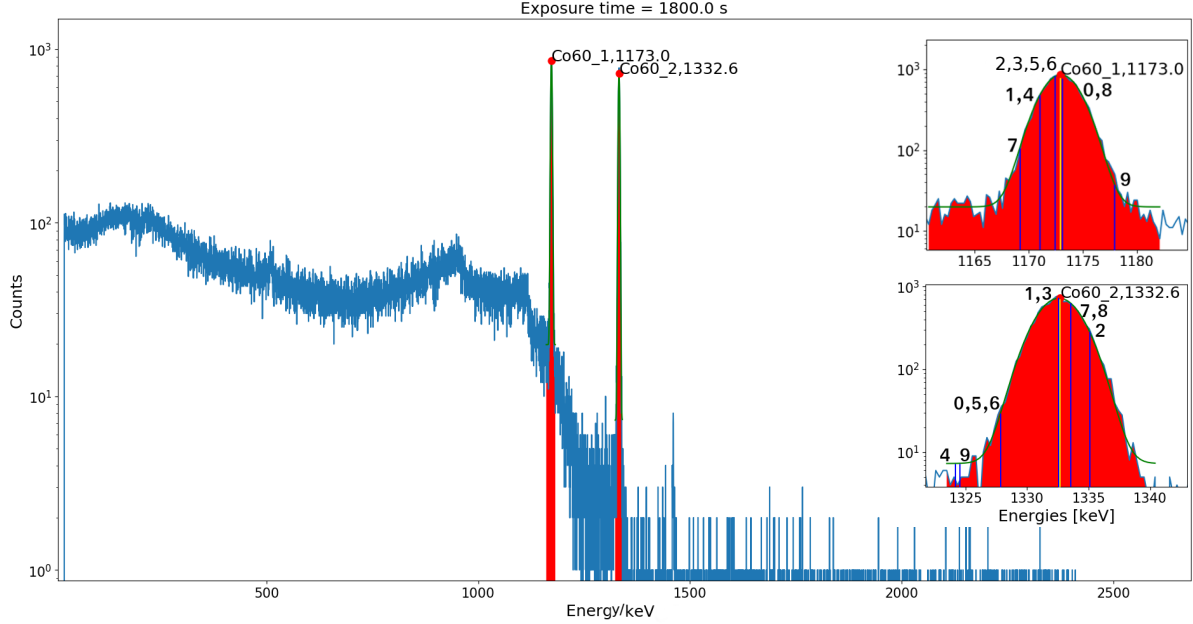


Fig. 5:  $^{60}\text{Co}$  spectrum obtained from the point-like source described in table III. Peak ranges for energy queries are drawn in red. Plot was made using `histoGe` [33]. The zoomed-in inserts show the peaks along with first 10  $\gamma$ -lines (tagged by their position) in accordance to table IV.

$$S_{\text{criterion}}(p_{\gamma\text{-line}}) = \begin{cases} 10 - p_{\gamma\text{-line}} & p_{\gamma\text{-line}} < 10 \\ 0 & p_{\gamma\text{-line}} \geq 10 \end{cases}, \quad (5)$$

where  $p_{\gamma\text{-line}}$  is the list position of the  $\gamma$ -line (starting from 0) for a given criterion. For example, in the  $^{109}\text{Cd}$  radioactive source (table V), the  $\gamma$ -line located at 88.04 keV was sorted

TABLE III: ENERGY AND HALF-LIFE OF THE POINT-LIKE SEALED SOURCES USED TO COMPARE RANKING CRITERIA.

ALL SOURCES HAD AN INITIAL ACTIVITY OF 1  $\mu\text{Ci}$  (EXCEPT  $^{137}\text{Cs}$  WITH 0.1  $\mu\text{Ci}$ , AS OF JANUARY 2019 AND A 20% UNCERTAINTY, AND  $^{241}\text{Am}$  WITH  $^{121}\text{In}$  AS OF AUGUST 1982).

Source	$\gamma$ -lines [keV]	half-life [yr]
$^{241}\text{Am}$	13.81, 27.03, 33.19, 43.42, 59.54, 69.76 98.97, 102.98, 120.36, 125.33	432.5
$^{133}\text{Ba}$	53.1, 79.6, 81.0, 160.6, 223.3, 276.3 302.8, 356.0, 383.8	10.5
$^{109}\text{Cd}$	88.07	1.27
$^{57}\text{Co}$	122.0, 136.0	0.745
$^{60}\text{Co}$	1173.2, 1332.5	5.27
$^{137}\text{Cs}$	662.0	30.1
$^{54}\text{Mn}$	835.0	0.855
$^{22}\text{Na}$	1275.0	2.6
$^{65}\text{Zn}$	1115.0	0.668

by criterion F at position 2 (third place) and it receives a score of  $10 - 2 = 8$ .

Then, the following operation is done for obtaining the normalized score (NS) for a specific criterion:

$$NS_{\text{criterion}} = \frac{\sum_{\gamma\text{-line}} S_{\text{criterion}}(p_{\gamma\text{-line}})}{MS} \quad (6)$$

where the maximum possible score is given by  $MS = 10 \times \text{Total}_{\gamma\text{-lines}} = 10 \times 27 = 270$ . The NS range is between 0 and 1, being 0 and 1 the worst and the best possible results, respectively.

Under these expressions, criterion B performed poorly (the expected  $\gamma$ -line positions are mostly above 9), it was taken as the baseline criteria during comparison with other methods. This means that coincidence probability is not relevant because it depends on a good calibration and its uncertainty. The fact that the density of  $\gamma$ -lines is so high affects the performance, because many other  $\gamma$ -lines could be as near as or nearer than that of interest. Criterion E was capable to identify  $^{133}\text{Ba}$  and  $^{60}\text{Co}$  but showed a poor performance for  $^{241}\text{Am}$  because it has 171  $\gamma$ -lines in [39] and 132  $\gamma$ -lines in the range of its spectrum but only 22  $\gamma$ -lines were observed. Criterion F improves the results obtained with the criterion E. In the worst case, it equals the performance of criterion E, but the fact that it uses the REP makes it able to focus on those  $\gamma$ -lines that



TABLE IV: THE ENERGY, GAMMA INTENSITY, PARENT ISOTOPE AND RANK VALUE FOR THE TOP 10 ISOTOPES FOUND IN EACH OF THE 2 QUERY RANGES (Co60\_1, Co60\_2), OBTAINED FROM RUNNING CRITERION F ON THE  $^{60}\text{Co}$  SEALED SOURCE SPECTRUM. SEE TEXT FOR DETAILS.

Co60 <sub>1</sub> : from 1160.84 to 1182.18 PBR = 8.2				
Eg [keV]	Ig (%)	Parent	Rank Value	Position
1173.237 (4)	99.97	$^{60}\text{Co}$	1.000	0
1171.3 (2)	1.70	$^{120}\text{Sb}$	0.889	1
1172.9 (1)	98.00	$^{62m}\text{Co}$	0.806	2
1172.9 (1)	98.00	$^{62m}\text{Co}$	0.806	3
1171.3 (2)	19.00	$^{120}\text{In}$	0.731	4
1172.9 (1)	84.00	$^{62}\text{Co}$	0.722	5
1172.9 (1)	0.34	$^{62}\text{Cu}$	0.579	6
1168.8 (5)	100.00	$^{128m}\text{Sn}$	0.491	7
1173.237 (4)	0.26	$^{60}\text{Cu}$	0.442	8
1178.5 ( )	64.00	$^{34}\text{Si}$	0.400	9
Co60 <sub>2</sub> : from 1323.41 to 1340.54 PBR = 24.4				
Eg [keV]	Ig (%)	Parent	Rank Value	Position
1332.501 (5)	99.99	$^{60}\text{Co}$	1.000	0 <sup>†</sup>
1328.2 (3)	5.60	$^{53}\text{Co}$	1.000	1
1335.04 (10)	71.00	$^{125}\text{In}$	0.693	2
1332.501 (5)	88.00	$^{60}\text{Cu}$	0.442	3
1324.1 (2)	0.47	$^{210}\text{At}$	0.347	4
1328.2 (3)	86.00	$^{53m}\text{Co}$	0.305	5
1328.2 (3)	87.00	$^{53m}\text{Fe}$	0.304	6
1333.4 (3)	0.52	$^{142}\text{Cs}$	0.221	7
1333.4 (3)	0.52	$^{142}\text{Cs}$	0.221	8
1324.51 (6)	17.50	$^{150}\text{Pm}$	0.192	9

have the highest EP giving little importance to those  $\gamma$ -lines that could be undetectable with a certain detector. Criterion H gave the best results, in particular, when those isotopes with a relatively small REP are filtered to discard them from sorting and ranking (H+). Fuzzy ranking is able to get approximately 0.95 or 0.87 of the maximum score with and without filtering (H and H+), respectively. The overall performance of H+ makes it the best one with a score of 0.955. This result suggests that combining the criteria to make identification algorithms can give better results than using individual criteria alone. For criterion J, fair results were obtained. A simple inspection of the results reveals that this criterion correctly identifies the  $\gamma$ -lines 7 of the 10 radioactive sources in Table I. In particular, the  $\gamma$ -lines for  $^{241}\text{Am}$  all get ranked at positions higher than 34 and the line of  $^{54}\text{Mn}$  was placed at position 251. In general,  $^{241}\text{Am}$  was hard to be identified by `histoGe` and this penalizes some criteria more than others.

Nonetheless, no significant improvements were observed when efficiency corrected spectra were used as input. Therefore, identification could be achieved without knowing the detector's efficiency [44]. Besides, a test was implemented to find the dependence of the ranking results against the peak-to-background ratio (PBR) defined as the ratio of the area enclosed by a peak to the area of the background beneath it, in an interval  $\pm 3\sigma$  around the peak, and calculated using an exponential plus second order polynomial fit. Fake peaks with variable amplitude were introduced in known spectra and it was found that, once the PDA detect the peak, the position of that  $\gamma$ -line is unaffected for methods E, F and J, and negligible changes in position were observed for B, H and H+. Thus,

identification of peaks with low PBR are not affected.

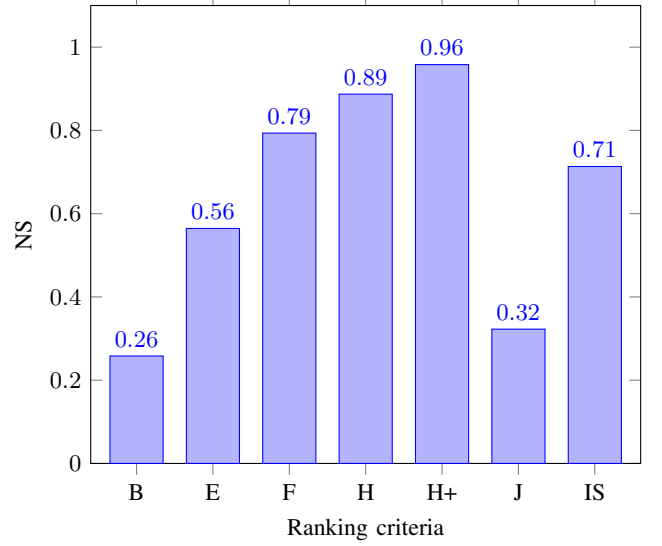


Fig. 6: Comparison of the performance of the criteria in identifying the  $\gamma$ -lines present in the point-like sources of Table III and an extended  $^{210}\text{Pb}$  source through the normalized score (NS) defined by (6). The score of InterSpec software [16] is shown in the last bar (IS).

### C. Performance over generic $\gamma$ spectra

To explore the capability of the program to identify isotopes in spectra that may contain an arbitrary combination of isotopes, various test were performed using previously studied samples [46], [47]: one had traces of  $^{210}\text{Pb}$  (sample A) and the other contained  $^{177}\text{Lu}$  and  $^{131}\text{I}$  (sample B) and a rock sample taken from the inside of LabChico's site (sample C). It was known that sample A was spiked with lead and it was acquired with the high purity germanium detector of the Institute of Physics of the UNAM (IF-BEGe detector) [44] with a exposure time of 24 h, spectrum of sample B was acquired inside the Boulby Underground Germanium Suite (BUGS) facility [48] at Boulby Underground Laboratory [49] and a previous analysis of sample B identified  $^{177}\text{Lu}$  and  $^{131}\text{I}$  [46] and sample C is a rock taken during geotechnical studies [47] and assayed with the ICN-UNAM HPGe [44].

Table VI shows the results of applying criteria F and H to samples A, B and C. Criteria F and H were chosen for this test because they showed the best performance in the test with the point-like sealed sources. For the sample A, in addition to the  $^{210}\text{Pb}$   $\gamma$ -line at 46.5 keV (positions 1 for rank F and 0 for rank H), two X-rays associated with  $^{210}\text{Pb}$  were observed, however, their assigned positions (higher than 20) are irrelevant because the database does not contain reliable information about X-rays. This motivates the addition of X-ray information to the LDB. For sample B, ranks H and H+ identified  $^{131}\text{I}$ ,  $^{177}\text{Lu}$  and  $^{40}\text{K}$  at positions 0 for all the  $\gamma$ -lines which is the best possible result. The  $^{40}\text{K}$  seen in sample B can be safely attributed to the water given the ultra low background of the BUGS detector [50]. About sample C,  $^{40}\text{K}$  was successfully

TABLE V: POSITION FOR EVERY  $\gamma$ -LINE EXPECTED FROM THE SPECTRA OF THE RADIOACTIVE SOURCES OF TABLE III USING THE CRITERIA DESCRIBED IN SECTION III. THE ISOTOPES AND THEIR  $\gamma$ -LINES PROPERTIES, ENERGY QUERY RANGE, THE NUMBER OF ISOTOPES FOUND IN THE QUERY RANGE, THE POSITIONS OF EACH  $\gamma$ -LINE ARE SHOWN FOR EACH CRITERION AND, BESIDES, THE IS'S INDIVIDUAL PERFORMANCE. THE TOP  $\gamma$ -LINE POSITION IS ZERO.  $^{210}\text{Pb}$  SPECTRA WAS OBTAINED FROM SAMPLE A FROM TABLE VI. FOR  $^{241}\text{Am}$  RANGES COULD INCLUDE MORE THAN ONE  $\gamma$ -LINE REPORTED IN THE DATABASE, IN THIS CASE ALL ARE RANKED TOGETHER.

	$\gamma$ -line Properties		Query Range		PBR	Size	$\gamma$ -line Position						
	Eg [keV]	Ig (%)	Emin	Emax			B	E	F	H	H+	J	IS
$^{241}\text{Am}$	26.344	2.4	24.187	28.355	10.5	200	0	75	7	1	1	34	4
	33.196	0.13	31.122	35.550	1.7	198	0	61	3	1	0	41	1
	43.423	0.07	42.355	44.483	0.2	143	1	50	5	5	0	29	9
	51.010	0.00	48.031	51.869	0.2	194	158	45	2	1	0	33	9
	59.541	35.9	56.673	63.802	19.5	414	0	114	9	3	1	82	1
	69.760	0.00	68.316	71.735	0.03	206	28	50	3	0	0	42	1
	75.800	0.00	75.411	78.530	0.1	177	153	53	5	4	2	39	9
	79.100	0.00	78.649	82.377	0.1	211	163	56	5	2	0	35	13
	98.970	0.02	96.695	100.024	0.5	251	17	81	1	5	0	44	4
	102.98	0.02	100.502	105.081	0.5	345	2	104	3	2	0	51	5
	120.36	0.00	116.561	121.999	2.9	372	198	124	4	1	1	24	4
	125.30	0.00	123.656	127.075	0.6	239	1	74	5	0	0	38	2
$^{133}\text{Ba}$	53.161	2.2	51.353	56.238	8.3	258	84	0	0	0	0	5	n/a
	79.613	2.62	78.327	84.538	5.1	344	206	1	1	0	0	8	3
	80.997	34.06	78.327	84.538	-	344	206	1	1	0	0	8	6
	160.613	0.65	156	166	0.06	681	61	0	0	1	1	9	0
	223.234	0.45	220	227	0.06	220	52	0	0	0	0	17	0
	276.398	7.16	273.776	279.103	7.5	273	41	0	0	0	1	10	2
	302.853	18.33	299.866	306.077	7.5	347	10	0	0	0	0	10	11
	356.017	62.05	352.929	360.140	197.6	382	11	0	0	0	0	4	0
$^{109}\text{Cd}$	88.04(5)	3.61	85.439	91.561	9.7	378	5	2	2	4	4	1	1
$^{57}\text{Co}$	122.0614	85.6	120.080	124.737	11.4	315	70	2	3	0	0	0	1
	136.474	10.68	135.534	138.000	17.2	135	52	2	2	0	0	0	2
$^{60}\text{Co}$	1173.237	99.97	1170.839	1176.184	8.2	222	28	0	0	0	0	0	0
	1332.501	99.99	1329.410	1336.537	24.4	89	2	0	0	0	0	0	0
$^{137}\text{Cs}$	661.657	85.1	660.302	663.393	13.0	142	2	1	1	1	1	0	0
$^{54}\text{Mn}$	834.848	99.98	831.232	838.346	19.1	343	61	0	0	0	0	251	0
$^{22}\text{Na}$	1274.53	99.94	1270.843	1277.957	22.2	253	14	0	0	0	0	0	0
$^{210}\text{Pb}$	46.539	4.25	45.704	47.067	0.9	68	31	1	1	0	0	1	1
$^{65}\text{Zn}$	1115.546	50.6	1101.568	1133.256	3.3	1151	12	5	1	4	1	4	0

identified by ranks F, H and H+. The photopeak observed at 2614 keV was attributed to  $^{208}\text{Tl}$  because it belongs to  $^{232}\text{Th}$  decay chain and was found at positions 3 for ranks F, H and H+. Two photopeaks were attributed to  $^{214}\text{Bi}$  because they belong to  $^{238}\text{U}$  decay chain, however, no further peaks that could have increased the confidence were identified due to the high background at energies below the potassium peak in the spectrum.  $^{214}\text{Bi}$  has 214 entries at the database but only two were considered resulting in a low REP which affected the behavior of H rank.

#### D. Ranking without raw data

It is often the case that the spectrum data is only available in image format and ranks E, F and J have the advantage of performing ranking without the raw data of the spectrum. To show this capability, a calibrated spectrum in which isotopes were identified and marked with tags (figure 2 of [51]) was analyzed using ranks F and J. The peak maxima and Full Width at Half Maximum reported (FWHM) were used to construct an info file [35] with 17 query ranges. The query ranges were defined as two times the FWHM except for  $^{234}\text{Th}$  in which only one FWHM was used. The positions and RV

for each  $\gamma$ -line are shown in Table VII. For rank F, all the  $\gamma$ -lines known to be present were placed within the first ten positions to explain the peak where they are found. 12 out of 17 were placed among the top three and 3 were positioned fourth. Criterion J placed the lines within the first ten positions except for  $^{234m}\text{Pa}$  and  $^{40}\text{K}$  which could not be associated with a specific decay chain in the LDB.

#### E. Comparison between histoGe and InterSpec

Table VIII shows a performance comparison between histoGe and InterSpec from Sandia Labs [16], whose output is also an ordered list. Two spectra were analyzed: sample B of Table VI and the background spectrum of the Lumpsey detector, at Boulby, (B-BKG) [50]. For sample B, rank H of histoGe outperforms InterSpec while rank F is slightly better, in particular, to identify  $^{177}\text{Lu}$  and the 80.185 keV photopeak of  $^{131}\text{I}$ . For B-BKG, InterSpec was capable of ranking correctly more  $\gamma$ -lines at first position in comparison to the best result of histoGe, however, there is one peak in which it fails completely ( $^{208}\text{Tl}$  at 510.77 eV) because it is confused with  $e^-e^+$  annihilation line. So, if  $\Delta$  is defined as the position difference between InterSpec



TABLE VI: POSITIONS AND RANKS, ACCORDING TO CRITERIA F, H AND H+, OF PARENT ISOTOPES KNOWN TO BE PRESENT IN THE TWO WATER SAMPLES (A AND B), AND AT THE INTENDED SITE FOR LABCHICO (C). THE QUERY RANGES AND  $\gamma$ -RAY PROPERTIES ARE ALSO SHOWN.  $^{214}\text{Bi}$  HAS 214  $\gamma$ -LINE AND DUE TO ONLY 2 LINES WERE IDENTIFIED, REP IS SMALL WHICH AFFECTS THE BEHAVIOR OF H RANK.

sample	isotope	$\gamma$ -ray properties		Query Range		PBR	Size	Position			RV		
		Eg [keV]	Ig (%)	Emin	Emax			F	H	H+	F	H	H+
A	$^{210}\text{Pb}$	46.53	4.25	45.70	47.06	0.950	69	1	0	0	1	0.873	0.873
B	$^{177}\text{Lu}$	112.94	6.4	111.11	115.14	1.010	279	1	0	0	0.965	0.904	0.999
	$^{177}\text{Lu}$	208.36	11.0	206.8	209.8	2.489	191	3	0	0	0.965	0.904	0.999
	$^{131}\text{I}$	80.18	2.62	79.3	82.0	0.169	158	4	0	0	0.969	0.912	0.999
	$^{131}\text{I}$	284.30	6.14	282.5	285.5	2.289	176	0	0	0	0.969	0.912	0.999
	$^{131}\text{I}$	364.48	81.7	362.51	366.1	11.321	189	0	0	0	0.969	0.912	0.999
	$^{131}\text{I}$	636.98	7.17	634.64	639.0	3.550	237	0	0	0	0.969	0.912	0.999
C	$^{40}\text{K}$	1460.83	11.0	1457.0	1463.53	541.346	158	0	0	0	1.000	0.873	0.873
	$^{214}\text{Bi}^*$	1693.3	0.01	1690.0	1694.0	0.106	88	1	19	0	0.117	0.120	0.468
	$^{214}\text{Bi}^*$	1764.49	15.4	1762.45	1766.96	0.383	92	3	19	1	0.117	0.120	0.468
	$^{208}\text{Tl}$	2614.5	99.0	2600	2620	0.957	150	3	3	3	0.432	0.417	0.674
	$^{40}\text{K}$	1460.83	11.0	1450.07	1467.09	0.436	423	0	0	0	1.000	0.873	0.873

TABLE VII: RV AND POSITIONS CALCULATED FOR 4 CRITERIA FROM THE PUBLISHED PARENT ISOTOPES ON FIGURE 2 OF [51]. NOTE FROM THE SIZE COLUMN THAT THE NUMBER OF CANDIDATES IS IN THE HUNDREDS.

isotope	$\gamma$ -line properties		Query Range [keV]		Size	Position		RV	
	Eg [keV]	Ig (%)	Emin	Emax		F	J	F	J
$^{210}\text{Pb}$	46.53	4.25	45.42	49.98	227	3	4	1	0.288
$^{234}\text{Th}$	63.29	4.8	62.34	64.20	127	9	1	0.188	0.288
$^{226}\text{Ra}$	187.1	-	184.2	188.20	278	2	4	0.333	0.288
$^{212}\text{Pb}$	238.63	43.3	236.64	241.97	306	1	5	0.912	0.218
$^{214}\text{Pb}$	351.93	37.6	349.9	353.9	265	5	4	0.536	0.288
$^{208}\text{Tl}$	583.2	84.5	581.20	585.27	219	1	8	0.801	0.218
$^{214}\text{Bi}$	609.31	-	607.30	611.35	225	2	0	0.581	0.288
$^{137}\text{Cs}$	661.65	85.1	659.7	663.7	198	1	5	1	0.255
$^{228}\text{Ac}$	911.20	25.8	909.21	913.26	182	2	9	0.383	0.181
$^{228}\text{Ac}$	968.97	15.8	967.27	971.03	155	0	7	0.383	0.181
$^{234m}\text{Pa}$	1001.03	0.84	999.02	1003.08	188	0	166	0.512	0
$^{214}\text{Bi}$	1120.2	15.1	1118.3	1122.35	151	1	3	0.581	0.288
$^{60}\text{Co}$	1173.23	99.0	1171.2	1175.2	176	0	0	1	0.499
$^{60}\text{Co}$	1332.5	99.0	1330.5	1334.5	360	0	0	1	0.499
$^{40}\text{K}$	1460.83	11.0	1458.8	1462.5	268	0	75	1	0
$^{214}\text{Bi}$	1764.49	15.4	1762.5	1766.5	85	0	1	0.581	0.288
$^{208}\text{Tl}$	2614.5	99.0	2612.5	2616.5	39	2	1	0.801	0.218

and the `histoGe`'s best result, it can be seen that  $\sum \Delta > 0$ , which means that `histoGe` had a better overall performance when both, sample B and B-BKGD are considered.

The paradigm by which `histoGe` identifies the isotopes is completely different in comparison to `InterSpec`'s. `histoGe` performs better when more photopeaks of an isotope are observed in the spectrum, however, sometimes `InterSpec` works better when individual peaks are considered in such a way that even identification of 2 unrelated peaks could make `InterSpec` fail the isotopes' identification unlike `histoGe` which is able to manage contextually many isotopes per run.

#### F. Computational cost

The computational cost of criteria F and H is due to querying the LDB, calculating the RV, and sorting all the  $\gamma$ -lines. A Monte Carlo analysis was performed to estimate the time used for these process. The procedure followed to implement this test is described next: `.info` files were randomly constructed with a variable number of  $\gamma$ -lines per file, and then, ranked. The center of the energy range was

chosen randomly between 200 keV and 2500 keV per each  $\gamma$ -line and its width was calculated using a distributed normally random numbers with  $\mu = 0$  and  $\sigma = 5$ . The minimum energy range is 1 keV to avoid small intervals that could contain few  $\gamma$ -lines. This procedure was repeated 100 times. The computer used to execute this analysis has a AMD Ryzen 7 processor 4800H, 16 GB of RAM and a SSD. A program was made to measure the execution time of each call to `histoGe` using those `.info` files generated randomly. For H criterion, an arbitrary spectrum was chosen considering that its energy range is larger than the query ranges. Figure 7 shows that the execution time follows a non-linear relationship in which increasing the number of peaks by 10 does not even get the execution time doubled. These results show that `histoGe` has reasonable ( $\geq 20s$ ) execution times for real spectra in which the number of  $\gamma$ -lines do not exceed a hundred peaks. As expected, H is slower than F, but for a low number of peaks, there is not a considerable difference between them.

On the other hand, note that processing a spectrum form peak identification using the PDA through the `histoGe`'s peak finder tool to  $\gamma$ -line identification using some criteria could take a few minutes, however, due to the peak finding

TABLE VIII: COMPARISON OF THE RESULTS OBTAINED BETWEEN HISTOGE VS. INTERSPEC (IS).  $\Delta$  MEANS THE DIFFERENCE OF POSITION OF INTERSPEC MINUS POSITION OF HISTOGE. A POSITIVE  $\Delta$  FAVORS HISTOGE. DUE TO  $^{214}\text{Bi}$  HAS MORE THAN 2 HUNDREDS OF PEAKS THE INFORMATION TO IDENTIFY IT CLEARLY IS INCOMPLETE MAKING HARDER THE IDENTIFICATION FOR HISTOGE.  $^{\dagger}$ RANGE HAD TO BE MADE WIDER SO IS COULD MAKE IDENTIFICATION.  $^{\ddagger}^{222}\text{Rn}$ ,  $e - e+$  AND  $^{214}\text{Pb}$  WERE IDENTIFIED AT POSITIONS 0, 1 AND 2, RESPECTIVELY AND BOTH ISOTOPES WERE FOUND IN THE BACKGROUND.

spectrum	Known isotope		Range		Position				$\Delta$
	isotope	Eg [keV]	Emin	Emax	F	H	H+	IS	
Sample B	$^{177}\text{Lu}$	112.94	111.1131	115.1425	1	0	0	1	1
	$^{177}\text{Lu}$	208.36	206.8	209.8	3	0	0	2	2
	$^{131}\text{I}$	80.18	79.3	82.0	4	0	0	6	6
	$^{131}\text{I}$	284.30	282.5	285.5	0	0	0	0	0
	$^{131}\text{I}$	364.48	362.51	366.1	0	0	0	0	0
	$^{131}\text{I}$	636.98	634.64	639.0	0	0	0	0	0
	$^{40}\text{K}$	1460.83	1457.0	1463.53	0	0	0	0	0
B-BKG	$^{214}\text{Bi}$	609.31	607.7	611.3	2	1	2	0	-1
	$^{214}\text{Bi}$	768.35	767.80	769.82	1	0	0	0	0
	$^{214}\text{Bi}$	1120.28	1119.10	1122.55	1	1	1	0	-1
	$^{214}\text{Bi}$	1764.49	1763.35	1767.20	1	1	1	0	-1
	$^{214}\text{Bi}$	2204.21	2203.50	2207.16	0	0	0	0	0
	$^{40}\text{K}$	1460.83	1459.5	1462.8	0	0	0	0	0
	$^{228}\text{Ac}$	911.20	909.7	913.16	1	1	2	0	-1
	$^{228}\text{Ac}$	968.97	967.57	971.23	0	0	0	0	0
	$^{228}\text{Ac}$	1588.19	1587.5	1589.77	0	0	0	0	0
	$^{212}\text{Pb}$	47.91	45.1	47.92	3	0	0	0 $^{\dagger}$	0
	$^{212}\text{Pb}$	238.63	237.00	239.95	0	0	0	0	0
	$^{212}\text{Pb}$	300.087	298.9	301.3	0	0	0	0	0
	$^{208}\text{Tl}$	510.77	509.82	512.16	2	3 $^{\ddagger}$	0	26	26
	$^{208}\text{Tl}$	583.19	581.8	584.89	1	2	1	0	-1
	$^{208}\text{Tl}$	860.56	859.2	862.5	0	0	0	0	0
	$^{208}\text{Tl}$	2614.53	2613.65	2617.31	1	2	0	0	0
	$^{214}\text{Pb}$	241.99	240.3	243.2	1	0	0	4	4
	$^{214}\text{Pb}$	295.22	293.76	296.3	0	1	0	0	0
	$^{214}\text{Pb}$	351.93	350.52	353.3	2	3	0	0	0

algorithms are not fully accurate more time could be required to adjust the query ranges in the `info` file by a trained spectroscopist.

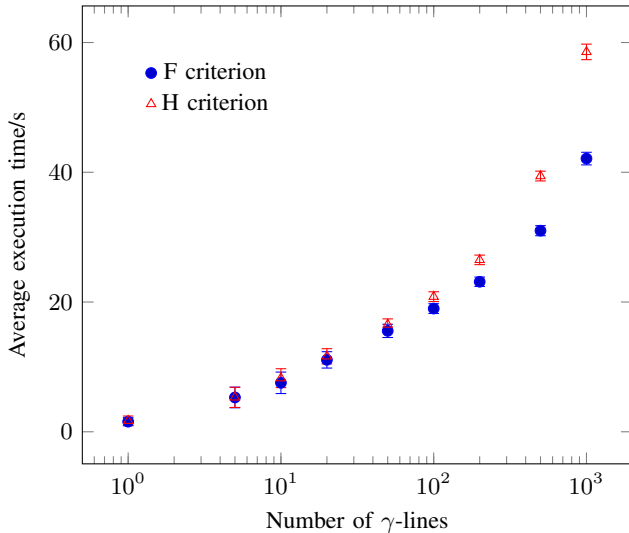


Fig. 7: Average and error bars ( $2\sigma$ ) of the execution time of criteria F (blue) and H (red) vs. the number  $\gamma$ -lines per info file.

## VI. CONCLUSIONS

histoGe is a tool for the identification of peaks in a  $\gamma$  spectrum using the information in a large database containing

92,453 gamma lines and 2,200 radioactive nuclides. The program implements different criteria to rank and sort candidate isotopes to explain the presence of peaks in a spectrum with a philosophy inspired by that of a search engine.

Five different criteria (III) were presented and their performances were compared according to their ability to identify the  $\gamma$ -lines from a suite of sealed calibrated radioactive gamma sources via an *ad hoc* defined metric. Two of the methods stood out in performance under this test: one based on the use of Relative Emission Probabilities (F), and one using fuzzy logic (H) which combine information used in other criteria. An enhanced version of the latter (H+) where  $\gamma$ -lines with relatively small REPs are discarded achieved  $\sim 95\%$  efficiency to identify the isotopes in a set of sealed radioactive sources. Under the same assumptions, InterSpec was also tested giving an efficiency of 70%, demonstrating that under this conditions histoGe performed better.  $^{241}\text{Am}$  was a hard isotope to identify, as only a small fraction of its  $\gamma$ -lines are typically visible in spectra. The score increases quite noticeably when  $^{241}\text{Am}$  is not considered.

histoGe was used to identify the  $\gamma$ -lines in three arbitrary samples: water with lead (sample A), London tap water (sample B) and the rock of LabChico's site (sample C). For sample A, a  $\gamma$ -line of  $^{210}\text{Pb}$  was identified with accuracy but X-rays were not because the database has not complete information about X-rays. For sample B, criterion H got the best score when  $^{177}\text{Lu}$ ,  $^{131}\text{I}$  and  $^{40}\text{K}$  were identified. For sample C,  $^{214}\text{Bi}$  was hardly identified by rank H due to it having 290  $\gamma$ -lines but rank F performed better and H+ identified it with accuracy.

An advantage of `histoGe` is that it is capable of making isotope identification using only the ranges of the photopeaks without the raw data of the spectrum. Criteria E, F, and J are capable of doing this. Then, a published spectrum was ranked with criterion F, it was capable to identify all of them within the 10 first positions, in fact most of them were among the first three places. Chain rank (III-E) identified all  $\gamma$ -lines in the top ten places except  $^{40}\text{K}$  and  $^{234\text{m}}\text{Pa}$  because there is not a decay chain associated with them. This result motivates further research about how to improve this rank.

`histoGe`'s results of identification of two samples were compared to those obtained with `InterSpec` of Sandia Labs. In general, the best result of `histoGe` outperformed `InterSpec`. Besides, from the results presented in section V-E and figure 6, it can be seen that `histoGe` is capable to make identification when multiple related or unrelated  $\gamma$ -lines are given at the same time, on the contrary, `InterSpec` cannot identify accurately unrelated peaks but is highly accurate in individual identification. These findings may change if both are tested under different conditions. Using the ideas presented in this work, a `histoGe` and `InterSpec` could be combined to get an even more accurate one.

From the Monte Carlo study, it was found that the computational cost for real spectra is affordable. The overall results have shown that `histoGe` is a tool capable to make reliable identification of isotopes through  $\gamma$ -spectroscopy with results comparable or even better than other similar software, which makes it able to be applied in teaching research and industrial applications. However, in its current state, we recommend that a trained spectroscopist analyze the results obtained with `histoGe` or `InterSpec` to get a better interpretation.

#### ACKNOWLEDGMENT

The authors would like to thank Prof. Peter Ekström (Lund University) and Prof. Dirk Rudolph (Lund University) for giving permission to use their database. We acknowledge the help of the Radiological Safety Unit of ICN-UNAM.

#### REFERENCES

- [1] G. Gilmore, *Practical gamma-ray spectroscopy*. John Wiley & Sons, 2011.
- [2] D. K. Fagan, S. M. Robinson, and R. C. Runkle, "Statistical methods applied to gamma-ray spectroscopy algorithms in nuclear security missions," *Applied Radiation and Isotopes*, vol. 70, no. 10, pp. 2428–2439, 2012.
- [3] C. Kalfas, M. Axiotis, and C. Tsabaris, "SPECTRW: a software package for nuclear and atomic spectroscopy," *Nuclear Instruments and Methods in Physics Research Section A: Accelerators, Spectrometers, Detectors and Associated Equipment*, vol. 830, pp. 265–274, 2016.
- [4] A. Simonits, J. Östör, S. Kálvin, and B. Fazekas, "HyperLab: A new concept in gamma-ray spectrum analysis," *Journal of Radioanalytical and Nuclear Chemistry*, vol. 257, no. 3, pp. 589–595, 2003.
- [5] M. Wasim, "GammaLab: a suite of programs for k 0-NAA and gamma-ray spectrum analysis," *Journal of radioanalytical and nuclear chemistry*, vol. 285, no. 2, pp. 337–342, 2010.
- [6] D. Arnold, M. Blaauw, S. Fazinic, and V. P. Kolotov, "The 2002 IAEA intercomparison of software for low-level  $\gamma$ -ray spectrometry," *Nuclear Instruments and Methods in Physics Research Section A: Accelerators, Spectrometers, Detectors and Associated Equipment*, vol. 536, no. 1–2, pp. 196–210, 2005.
- [7] S. P. Nielsen and S. E. Pålsson, "An intercomparison of software for processing Ge  $\gamma$ -ray spectra," *Nuclear Instruments and Methods in Physics Research Section A: Accelerators, Spectrometers, Detectors and Associated Equipment*, vol. 416, no. 2–3, pp. 415–424, 1998.
- [8] M. Blaauw, V. O. Fernandez, P. Van Espen, G. Bernasconi, R. C. Noy, H. M. Dung, and N. Molla, "The 1995 IAEA intercomparison of  $\gamma$ -ray spectrum analysis software," *Nuclear Instruments and Methods in Physics Research Section A: Accelerators, Spectrometers, Detectors and Associated Equipment*, vol. 387, no. 3, pp. 416–432, 1997.
- [9] G. S. Zahn, F. A. Genezini, and M. Morales, "Evaluation of peak-fitting software for gamma spectrum analysis," *arXiv preprint arXiv:1511.04362*, 2015.
- [10] M. M. Guilherme S. Zahn, Frederico A. Genezini, "Evaluation of peak-fitting software for gamma spectrum analysis," *arXiv:1511.04362v1*, 2015.
- [11] M. Wasim and J. Zaidi, "NUCDBA: a useful database for NAA lab," *Nuclear Instruments and Methods in Physics Research Section A: Accelerators, Spectrometers, Detectors and Associated Equipment*, vol. 481, no. 1–3, pp. 760–764, 2002.
- [12] R. F. S. Y. F. Chu, L. P. Ekström, "WWW Table of Radioactive Isotopes," <http://nucleardata.nuclear.lu.se/toi/>, 2019, database version 1999-02-28.
- [13] I. A. E. A. (IAEA), "Live chart of nuclides," <https://nds.iaea.org/relnsd/vcharthtml/VChartHTML.html>, 2020, accessed: 2020-06-03.
- [14] "National Nuclear Data Center," <https://www.nndc.bnl.gov/>, 2020, accessed: 2020-04-30.
- [15] V. Kolotov and V. Atrashkevich, "Software ASPRO-NUC: gamma-ray spectrometry, routine NAA, isotope identification and data management," *Journal of Radioanalytical and Nuclear Chemistry*, vol. 193, no. 2, pp. 195–206, 1995.
- [16] Sandialabs, "Interspec version 11.2.3," <https://github.com/sandialabs/InterSpec>, 2020.
- [17] —, "Peak-map," <https://github.com/sandialabs/Peak-Map>, 2020.
- [18] C. J. Sullivan, S. Garner, M. Lombardi, K. Butterfield, and M. Smith-Nelson, "Evaluation of key detector parameters for isotope identification," in *2007 IEEE Nuclear Science Symposium Conference Record*, vol. 2. IEEE, 2007, pp. 1181–1184.
- [19] H. Shahabinejad and N. Vosoughi, "Analysis of complex gamma-ray spectra using particle swarm optimization," *Nuclear Instruments and Methods in Physics Research Section A: Accelerators, Spectrometers, Detectors and Associated Equipment*, vol. 911, pp. 123–130, 2018.
- [20] D. Boardman and A. Flynn, "A gamma-ray identification algorithm based on Fisher linear discriminant analysis," *IEEE Transactions on Nuclear Science*, vol. 60, no. 1, pp. 270–277, 2012.
- [21] C. J. Sullivan and J. Stinnett, "Validation of a Bayesian-based isotope identification algorithm," *Nuclear Instruments and Methods in Physics Research Section A: Accelerators, Spectrometers, Detectors and Associated Equipment*, vol. 784, pp. 298–305, 2015.
- [22] J. Kim, K. T. Lim, J. Kim, Y. Kim, H. Kim, and G. Cho, "Quantification and uncertainty analysis of low-resolution gamma-ray spectrometry using bayesian inference," *Nuclear Instruments and Methods in Physics Research Section A: Accelerators, Spectrometers, Detectors and Associated Equipment*, vol. 953, p. 163144, 2020.
- [23] M. Kamuda and C. J. Sullivan, "An automated isotope identification and quantification algorithm for isotope mixtures in low-resolution gamma-ray spectra," *Radiation Physics and Chemistry*, vol. 155, pp. 281–286, 2019.
- [24] P.-L. Lagari, "An RBF neural network approach in radionuclide identification of unknown sources utilizing  $\gamma$ -ray spectra," Ph.D. dissertation, Purdue University, 2017.
- [25] M. Kamuda, J. Stinnett, and C. Sullivan, "Automated isotope identification algorithm using artificial neural networks," *IEEE Transactions on Nuclear Science*, vol. 64, no. 7, pp. 1858–1864, 2017.
- [26] J. Kim, K. Park, and G. Cho, "Multi-radioisotope identification algorithm using an artificial neural network for plastic gamma spectra," *Applied Radiation and Isotopes*, vol. 147, pp. 83–90, 2019.
- [27] A. Varley, A. Tyler, L. Smith, and P. Dale, "Development of a neural network approach to characterise  $^{226}\text{Ra}$  contamination at legacy sites using gamma-ray spectra taken from boreholes," *Journal of environmental radioactivity*, vol. 140, pp. 130–140, 2015.
- [28] M. Kamuda, J. Zhao, and K. Huff, "A comparison of machine learning methods for automated gamma-ray spectroscopy," *Nuclear Instruments and Methods in Physics Research Section A: Accelerators, Spectrometers, Detectors and Associated Equipment*, vol. 954, p. 161385, 2020.
- [29] L. F. Blázquez, F. Aller, S. Vrublevskaia, J. Fombellida, and E. Valtuille, "Classification of radionuclides on polyvinyl toluene radiation portal monitors by a neural network based system §," *IFAC-PapersOnLine*, vol. 48, no. 21, pp. 852–857, 2015.
- [30] M. Alamaniotis and T. Jevremovic, "Hybrid fuzzy-genetic approach integrating peak identification and spectrum fitting for complex gamma-ray spectra analysis," *IEEE Transactions on Nuclear Science*, vol. 62, no. 3, pp. 1262–1277, 2015.

- [31] J. B. Stinnett, "Automated isotope identification algorithms for low-resolution gamma spectrometers," Ph.D. dissertation, University of Illinois at Urbana-Champaign, 2016.
- [32] A. Turner, C. Wheldon, M. Gilbert, L. Packer, J. Burns, T. K. Wheldon, and M. Freer, "Generalised gamma spectrometry simulator for problems in nuclide identification," *Journal of Physics: Conference Series*, vol. 1643, p. 012211, dec 2020. [Online]. Available: <https://doi.org/10.1088/1742-6596/1643/1/012211>
- [33] "histoGe v2.1," <https://doi.org/10.5281/zenodo.6339690>, 2022, accessed: 2022-03-08.
- [34] "GNU general public license," <http://www.gnu.org/licenses/gpl.html>, Free Software Foundation.
- [35] "histoGe User's Manual," <https://doi.org/10.5281/zenodo.6339653>, 2022, accessed: 2022-03-08.
- [36] "Comarca Minera Hidalgo UNESCO global geopark," 2020, <https://www.geoparquehidalgo.com>.
- [37] G. Van Rossum and F. L. Drake, *Python 3 Reference Manual*. Scotts Valley, CA: CreateSpace, 2009.
- [38] A. Savitzky and M. J. E. Golay, "Smoothing and differentiation of data by simplified least squares procedures," *Anal. Chem.*, vol. 36, no. 8, pp. 1627–1639, 1964.
- [39] "Database used with histoGe," <https://zenodo.org/record/4437341>, 2021, accessed: 2021-01-13.
- [40] L. A. Zadeh, "Fuzzy logic," *Computer*, vol. 21, no. 4, pp. 83–93, 1988.
- [41] T. J. Ross, *Fuzzy logic with engineering applications*. John Wiley & Sons, 2005.
- [42] L. A. Zadeh, "Fuzzy sets," *Information and control*, vol. 8, no. 3, pp. 338–353, 1965.
- [43] E. H. Mamdani, "Advances in the linguistic synthesis of fuzzy controllers," *International Journal of Man-Machine Studies*, vol. 8, no. 6, pp. 669–678, 1976.
- [44] A. Aguilar-Arevalo, S. Alvarado-Mijangos, X. Bertou, C. Canet, M. Cruz-Pérez, A. Deisting, A. Dias, J. D'Olive, F. Favela-Pérez, E. Garcés, A. G. Muñoz, J. Guerra-Pulido, J. Mancera-Alejandrez, D. Marín-Lámbarri, M. M. Montero, J. Monroe, C. I. Ortega-Hernández, S. Paling, S. Peeters, D. R. E. Rodríguez, P. Scovell, C. Türkoğlu, E. Vázquez-Jáuregui, and J. Walding, "Characterization of germanium detectors for the first underground laboratory in Mexico," *Journal of Instrumentation*, vol. 15, no. 11, pp. P11014–P11014, nov 2020. [Online]. Available: <https://doi.org/10.1088/1748-0221/15/11/P11014>
- [45] "Amptek materials analysis division," 2020, <https://www.amptek.com>.
- [46] A. Aguilar-Arevalo, X. Bertou, C. Canet Miquel, M. A. Cruz-Pérez, A. Deisting, A. Dias, J. C. D'Olive, F. Favela-Pérez, E. A. Garcés, A. González Muñoz, J. O. Guerra-Pulido, J. Mancera-Alejandrez, D. Marín-Lámbarri, M. Martínez Montero, J. R. Monroe, C. I. Ortega-Hernández, S. Paling, S. Peeters, D. Ruíz Esparza Rodríguez, P. R. Scovell, C. Türkoğlu, E. Vázquez-Jáuregui, and J. Walding, "Volume reduction of water samples to increase sensitivity for radioassay of lead contamination," April 2022, accepted for publication in *Water Applied Science*.
- [47] A. Aguilar-Arevalo, X. Bertou, C. Canet, M. A. Cruz, A. Deisting, A. Dias, J. C. D'Olive, F. Favela-Pérez, E. A. Garcés, A. González Muñoz, J. O. Guerra-Pulido, D. Marín-Lámbarri, A. M. Martínez Mendoza, M. Martínez Montero, J. Monroe, S. Paling, S. Peeters, P. R. Scovell, C. Türkoğlu, I. G. Vallejo Castillo, E. Vázquez-Jáuregui, and J. Walding, "Gamma-ray flux measurement and geotechnical studies at the selected site for the labchico underground laboratory," *The European Physical Journal Plus*, vol. 137, no. 2, pp. 1–11, 2022.
- [48] P. Scovell, E. Meehan, H. Araújo, J. Dobson, C. Ghag, H. Kraus, V. Kudryavtsev, X.-R. Liu, P. Majewski, S. Paling, R. Preece, R. Saakyan, A. Tomás, C. Toth, and L. Yeoman, "Low-background gamma spectroscopy at the Boulby Underground Laboratory," *Astroparticle Physics*, vol. 97, pp. 160 – 173, 2018. [Online]. Available: <http://www.sciencedirect.com/science/article/pii/S0927650517302517>
- [49] D. Malczewski, J. Kisiel, and J. Dorda, "Gamma background measurements in the Boulby Underground Laboratory," *Journal of Radioanalytical and Nuclear Chemistry*, vol. 298, no. 3, pp. 1483–1489, Dec 2013. [Online]. Available: <https://doi.org/10.1007/s10967-013-2540-9>
- [50] P. Scovell, E. Meehan, H. Araújo, J. Dobson, C. Ghag, H. Kraus, V. Kudryavtsev, P. Majewski, S. Paling, R. Preece *et al.*, "Low-background gamma spectroscopy at the Boulby underground laboratory," *Astroparticle Physics*, vol. 97, pp. 160–173, 2018.
- [51] S. Das, S. Ghorui, P. Raina, A. Singh, P. Rath, F. Cappella, R. Cerulli, M. Laubenstein, P. Belli, and R. Bernabei, "Preliminary study of feasibility of an experiment looking for excited state double beta transitions in tin," *Nuclear Instruments and Methods in Physics Research Section A: Accelerators, Spectrometers, Detectors and Associated Equipment*, vol. 797, pp. 130–137, 2015.